The effect of lesion size and tissue remodeling on ST deviation in partial-thickness ischemia

Mark Potse, PhD,*† Ruben Coronel, MD, PhD,‡ Stéphanie Falcao, MSc,*§ A.-Robert LeBlanc, PhD,*† Alain Vinet, PhD*†

*From the *Research Center, Sacré-Coeur Hospital, and †Institute of Biomedical Engineering, Université de Montréal, Montréal, Québec, Canada, ‡Experimental Cardiology Department, Academic Medical Center, University of Amsterdam, The Netherlands, and §Department of Pharmacology, Université de Montréal, Montréal, Québec, Canada.*

BACKGROUND Myocardial ischemia causes ST segment elevation or depression in electrocardiograms and epicardial leads. ST depression in epicardium overlying the ischemic zone indicates that the ischemia is nontransmural. However, nontransmural ischemia does not always cause ST depression. Especially in animal models, ST depression is hard to reproduce.

OBJECTIVE The purpose of this study was to determine the circumstances in which ST depression could be expected.

METHODS We studied ischemia in a large-scale computer model of the human heart. A realistic representation of the ischemia-induced changes in resting membrane potential was used, which was based on diffusion of extracellular potassium. Ischemia diameter, transmural extent, and tissue conductivity were varied.

RESULTS Our simulations confirm earlier work showing that partial-thickness ischemia, like full-thickness ischemia, typically causes ST elevation in an anisotropic model of the ventricles. However, we identified three situations in which ST depression can occur in overlying leads. The first is a reduced anisotropy ratio of the intracellular conductivity, which may result from hypertrophy and gap-junctional remodeling, circumstances that are likely to accompany ischemia. Second, an increase of the extracellular anisotropy has the same effect. Third, ST depression was found, independent of the anisotropy ratios, in very large and thin ischemic regions, resembling those that may occur in left-main or multivessel disease.

CONCLUSION Both tissue remodeling and geometric factors can explain ST depression in overlying epicardial leads. We note at the same time that ST elevation is found in most circumstances, while depression occurs as a reciprocal effect, even in partial-thickness ischemia.

KEYWORDS Ischemia; ST deviation; NSTEMI; Gap junctions; Tissue remodeling; Computer model; Extracellular potassium

(Heart Rhythm 2007;4:200–206)

Introduction

Myocardial ischemia can cause elevation and depression of the ST segment in electrocardiograms (ECGs) and epicardial electrograms. Elevation is a sign of myocardial infarction due to complete occlusion of a coronary artery.[1] Depression, especially in leads proximal to the occluded artery,[2–6] is related to incomplete occlusion and is thought to be mediated by subendocardial ischemia.[7,8]

In ischemic tissue the resting membrane potential (V_m) is depolarized with respect to normal tissue. This leads to a depression of the TQ segment in the local extracellular electrogram.[9–11] With the customary AC-coupled amplifiers, the TQ segment must be defined as isoelectric, so the change is observed as an elevation of the ST segment. In addition, true ST elevation can develop in advancing ischemia because of a reduction of action potential amplitude and duration.[12] For convenience, we describe both TQ and ST changes as ST segment deviations.

Elevation of the ST segment is observed in epicardial leads overlying a transmural ischemia.[12] Depression in overlying leads can only occur in partial-thickness ischemia.[13] In epicardial leads, ST depression has been observed when subendocardial ischemia or injury was produced in the *in situ* dog heart.[11,13] These studies suggested that the ST depression area on the epicardium coincided with the ST elevation area on the endocardium. However, in other studies the deepest ST depression was located over a lateral border of the ischemia,[14,15] and the negative zone on the epicardium did not move during a transition from partial-thickness to full-thickness ischemia.[15] Thus, partial-thickness ischemia alone cannot explain ST depression.

Recent computer simulations have predicted ST elevation in epicardial leads overlying a partial-thickness ischemia,[16,17] while ST depression was found adjacent to the

Computational resources for this work were provided by the Réseau québécois de calcul de haute performance (RQCHP). M. Potse was supported by a postdoctoral award from the Groupe de recherche en simulation et technologie biomédical (GRSTB), École Polytechnique and Université de Montréal; and by the Research Center of Sacré-Coeur Hospital, Montréal, Québec, Canada. **Address reprint requests and correspondence:** Dr. M. Potse, Research Center, Sacré-Coeur Hospital, K-3005, 5400 Boulevard Gouin Ouest, Montréal, Québec H4J 1C5, Canada. E-mail address: mark@potse.nl. (Received July 26, 2006; accepted October 13, 2006.)

1547-5271/$ -see front matter © 2007 Heart Rhythm Society. All rights reserved. doi:10.1016/j.hrthm.2006.10.022

ischemic area. These studies were based on realistic conductivity values for healthy myocardium. However, ischemic myocardium is likely to have been ischemic before or to show other symptoms of heart failure. Its conductivity may be modified because of hypertrophy and redistribution of gap junctions.[18–24]

The distinction between ST elevation and ST depression is central to the analysis of ECG changes in patients with acute coronary syndromes. Therefore, a good understanding of the mechanisms underlying ST elevation/depression is required. Understanding of the epicardial ST deviations that are observed in experimental models provides an important part of the overall picture. In this study, we use a computer model of the human heart with a realistic representation of the ischemic zone to identify the factors that can account for ST depression in leads overlying a subendocardial ischemic area.

Methods

Extracellular potentials were simulated with a computer model of the human heart that has been described elsewhere.[25] Briefly, the heart was discretized in three dimensions at 0.25-mm resolution. Extracellular potentials were computed at 22 million nodes connected with an anisotropic bidomain tissue model[26,27] incorporating a transmural fiber rotation. Since we were only interested in the amount of ST deviation, we did not simulate propagation. Instead, we used a fixed distribution of resting V_m. The model then computed the corresponding extracellular potentials.

The V_m pattern was based on a computed distribution of extracellular K^+ concentration ($[K^+]_o$). To obtain this distribution, we assumed that in ischemic myocardium K^+ is extruded from the cells at a rate of 13 μM/s[28,29] while normal, perfused myocardium maintains its $[K^+]_o$ near 5 mM. A discrete boundary between normal and ischemic regions was used to represent the very narrow metabolic border.[30–32] In addition, we reckoned that K^+ diffuses through the myocardium even in ischemic regions.[28] The distribution of $[K^+]_o$ can then be described by a diffusion equation[33] with source term S:

$$(1) \quad \frac{\partial[K^+]_o}{\partial t} = D\nabla^2[K^+]_o + S,$$

where D is the apparent diffusion constant of the tissue for K^+ ions

$$(2) \quad S = 13\ \mu\text{M/s} \text{ for ischemic myocardium and}$$

$$(3) \quad S = g \cdot (5\text{ mM} - [K^+]_o) \text{ elswhere,}$$

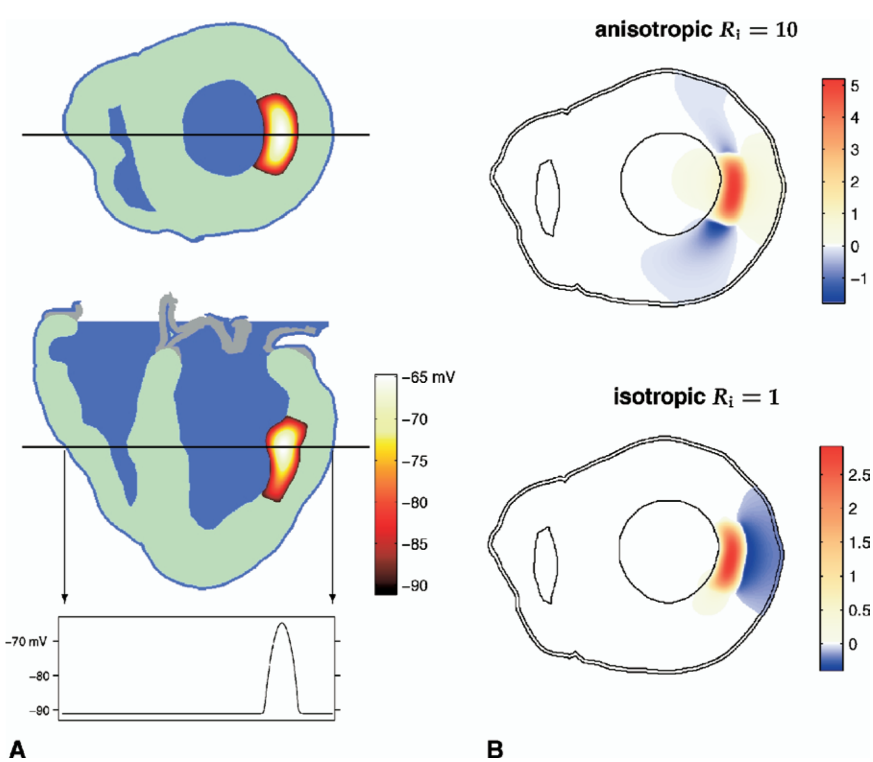

Figure 1 **A:** Transverse and longitudinal sections of the model anatomy, with normal myocardium shown as *green*, blood as *blue*, and connective tissue as *gray*. The horizontal line in each slice indicates where the other slice was taken. A color scale from black through red to white indicates resting V_m in the ischemic region, ranging from −91 to −65 mV. The normal myocardium, although shown in a different color, has the same resting potential of −91 mV as the very border of the ischemic zone. The ischemic region in this example had diameter d = 30 mm and extent e = 50%. The V_m profile along the line shown in the *upper two panels* is depicted in the *lower panel*. The profile is approximately parabolic with a slightly rounded foot. **B:** ST deviations in the extracellular domain. Potential differences are shown as pseudocolors; the scale is in millivolts. *Upper panel*: normal R_i = 10. *Lower panel*: isotropic intracellular domain. In the normal anisotropic case, ST elevation is measured on the epicardium. In the isotropic case, ST depression is obtained. Because of the anisotropy of the extracellular domain and the conductivity of the cavitary blood, the epicardium is then more negative than the endocardium adjacent to the ischemia. The geometry of the ischemic region is shown in panel **A**.

Table 1 Assumed normal bidomain conductivity values in units of milliSiemens/cm.

	Transverse	Longitudinal	Ratio	Reference
Intracellular	$\sigma_{iT} = 0.3$	$\sigma_{iL} = 3.0$	$R_i = 10$	36
Extracellular	$\sigma_{eT} = 1.2$	$\sigma_{eL} = 3.0$	$R_e = 2.5$	36
Blood	Isotropic $\sigma_e = 6.0$			54
Connective tissue	Isotropic $\sigma_e = 2.0$			

The value for connective tissue is an estimate based on the value for the human trunk.[54]

where g is a constant that describes the capacity of the perfusion to remove K^+ from the extracellular space. Expression (3) was applied in the normal myocardium, connective tissue, and intracavitary blood. Since both D and g are unknown, we chose $g = 5\ s^{-1}$ and scaled D such that $[K^+]_o$ in the center of the ischemic zone was 14 mM. No-flow boundary conditions were used at the tissue-air and blood-air interfaces (Figure 1**A**). By integrating equation (1) through time until a stable state was reached, we obtained a distribution of $[K^+]_o$ throughout the heart. Using a mathematical model of the human ventricular cell membrane,[34] we translated the $[K^+]_o$ value into a V_m for each node. The influence of V_m on the K^+ extrusion rate was ignored.

By considering only changes in resting V_m, we simulated TQ segment changes. For convenience, we will describe these as apparent ST segment changes. True ST segment changes (due to changes in action potential duration and plateau potential) were ignored. This should not affect our results in a significant way because the effects of true ST segment changes only amplify those of the apparent ST segment changes.

A subendocardial ischemic region was assumed in the lateral wall of the left ventricle. Several different geometries were explored, characterized by a diameter d (in millimeters) and a transmural extent e given as a percentage. An example of such a region and the computed offsets in resting V_m are shown in Figure 1**A**.

The bidomain model represents the myocardium by two co-located syncytia, called the "intracellular domain" and "extracellular domain," each characterized by anisotropic conductivities (Table 1). The intracellular domain represents the cells and gap junctions, while the extracellular domain represents the interstitium and small blood vessels.[35] The anisotropy ratios of the conductivities of the two domains will be denoted by R_i and R_e, respectively. To implement gap-junctional remodeling with the bidomain model, we varied R_i stepwise around its normal value of 10 by modifying the longitudinal conductivity (σ_{iL}). Intracavitary blood and connective tissue were isotropic and had no intracellular domain.

Results

Figure 1**B** shows simulated extracellular potentials in a section of the heart. In a normal anisotropic intracellular domain, injury current flows mainly along the fibers. This creates two current sinks in the extracellular domain adjacent to the ischemic area and a positive area on the epicardial side, as explained previously by Hopenfeld et al.[16] On the epicardium directly overlying the center of the ischemic area, the extracellular potential is positive.

In contrast, in a fully isotropic intracellular domain, current flows equally in all directions. This leads to a current sink area in the extracellular domain surrounding the ischemic area. The epicardium overlying the ischemia now shows a negative potential. The anisotropy of the extracellular domain makes the overlying epicardium more negative than the endocardium adjacent to the ischemia. This effect is enhanced by the intracavitary blood.

The results shown above apply to the two extreme cases: normal anisotropic ($R_i = 10$) and isotropic ($R_i = 1$). We also investigated intermediate anisotropy ratios. The ST deviation measured on the epicardium in the center of the ischemic region is shown in Figure 2. The ST deviation is seen to reduce gradually with a reduction in anisotropy ratio and to become negative when $R_i \leq 3$. The analysis was repeated with the intracavitary blood removed. In this case, the ST elevations were much larger and reversal occurred only at $R_i \leq 2.5$. All further experiments were performed with blood-filled cavity.

The effect of transverse conductivity was also investigated. In Figure 3, the ST deviation is again considered as a function of R_i for two different values of transverse con-

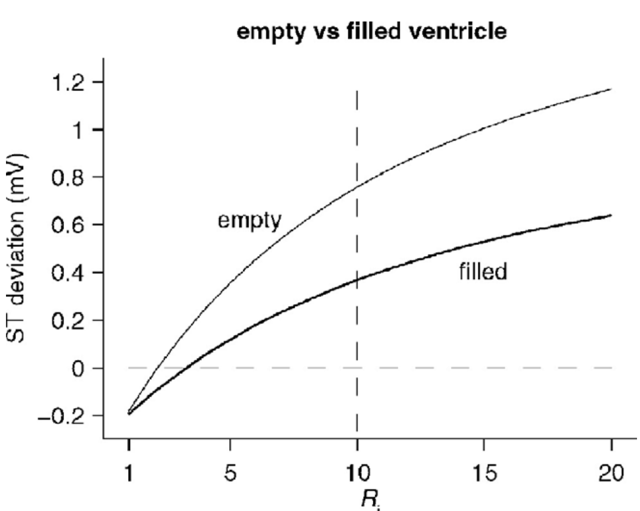

Figure 2 ST deviation on the epicardium in the center of the ischemic region as a function of R_i. *Thick line*: blood-filled cavities; *thin line*: empty cavities. In the blood-filled heart, transition from ST elevation to ST depression occurs when $R_i \leq 3$. In an empty heart, the transition occurs when $R_i \approx R_e$, i.e., at 2.5 (Table 1). The vertical line marks the assumed normal $R_i = 10$. The geometry of the ischemic region was $d = 30$ mm and $e = 50\%$, as in Figure 1**A**.

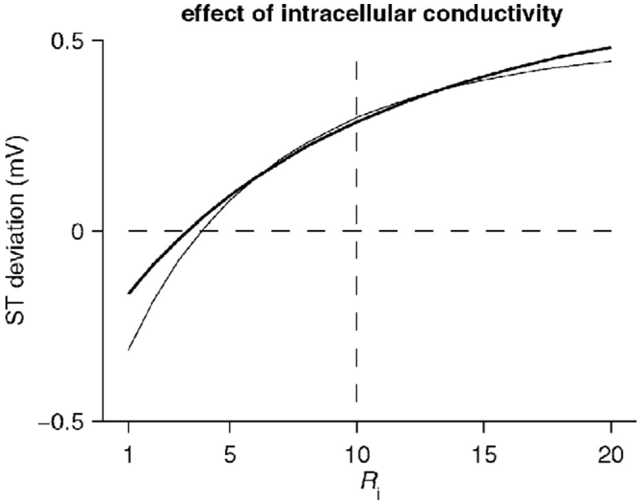

Figure 3 Effect of conductivity in the intracellular domain. The ST deviation is shown as a function of R_i. *Thick line*: $\sigma_{iT} = 0.3$; *thin line*: $\sigma_{iT} = 0.6$ mS/cm. The geometry of the ischemic region was $d = 30$ mm and $e = 50\%$. By itself, σ_{iT} turns out to have little effect; the anisotropy ratio is the primary determinant of ST deviation.

ductivity. The two curves are nearly coincident, demonstrating that conductivity changes without change in anisotropy ratio have only a limited effect; increased conductivity increases ST depression notably at low R_i. The anisotropy ratio is the main determinant of the sign of ST deviation.

The anisotropy ratio of the extracellular domain, R_e, also affects ST deviation, as shown in Figure 4. Increased R_e decreases ST elevation and increases ST depression. In the presence of a doubled R_e, a slightly reduced value of $R_i = 7$ would already cause ST depression.

Figure 5 shows the effect of ischemic geometry on the epicardial ST deviation. It demonstrates that larger diameter and smaller transmural extent favor ST depression. Depression is obtained for all tested R_i when $d = 75$ mm and $e \leq 30\%$. This corresponds to a thin ischemic area that covers more than half of the left ventricular endocardium. With a larger diameter, the magnitude of the ST deviation can be larger.

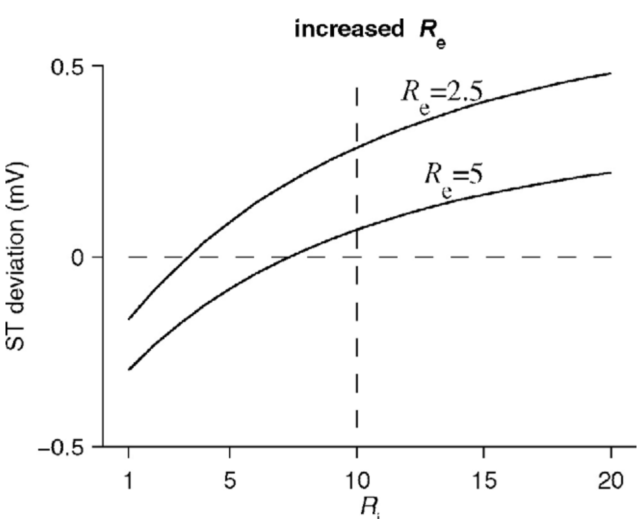

Figure 4 Effect of increased R_e. The ST deviation is shown as a function of R_i. *Upper curve*: normal $R_e = 2.5$ ($\sigma_{eT} = 1.2$, $\sigma_{eL} = 3.0$), as in Figure 2. *Lower curve*: increased $R_e = 5.0$ due to a reduced transverse component ($\sigma_{eT} = 0.6$, $\sigma_{eL} = 3.0$). The geometry of the ischemic region was $d = 30$ mm and $e = 50\%$.

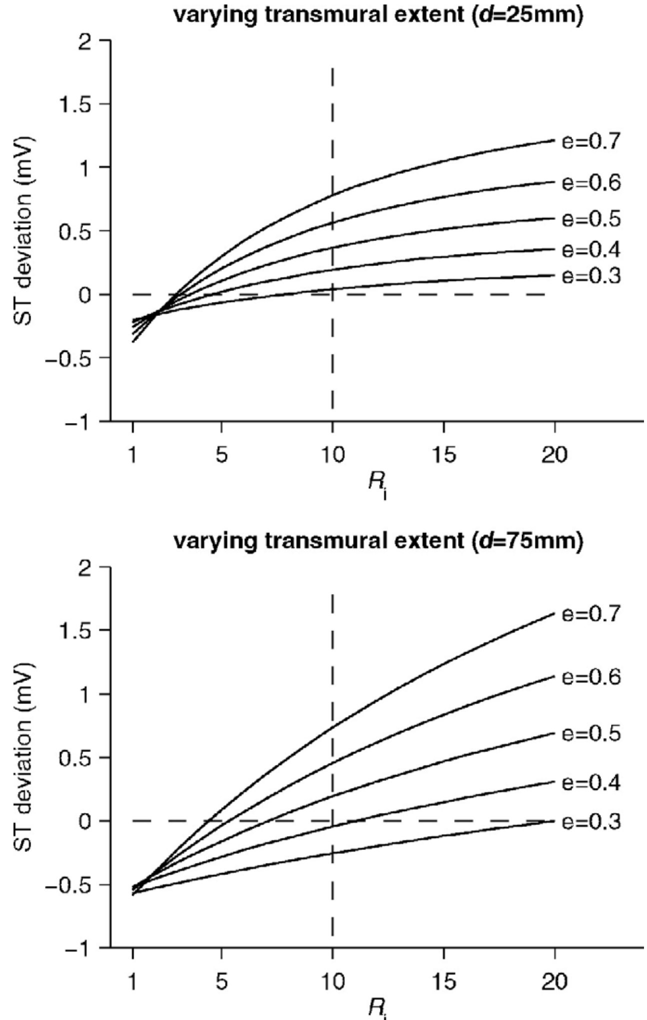

Figure 5 Effect of diameter and extent of the ischemic region. The ST deviation is shown as a function of R_i. In the *upper panel*, the diameter is fixed at 25 mm, while the transmural extent is varied from 30% to 70%. For every extent value, ST depression is found when the intracellular domain is nearly isotropic. The range of anisotropy values for which ST depression is obtained is larger for thinner ischemic regions. In the *lower panel*, the diameter is 75 mm, and the same values of transmural extent are shown. The relation between anisotropy ratio and ST deviation is similar to the 25-mm case, but the curves are steeper and, more importantly, shifted downward. For this diameter, ST depression can be obtained with normal anisotropy and a transmural extent of 30%.

Discussion

The classical theory of ST depression overlying an ischemic zone is often illustrated with a cartoon such as the one shown in Figure 6**A**. Recent experimental and theoretical studies, however, showed elevation in overlying epicardium.[14–17] The reason for the discrepancy is that the classical theory does not account for anisotropy.

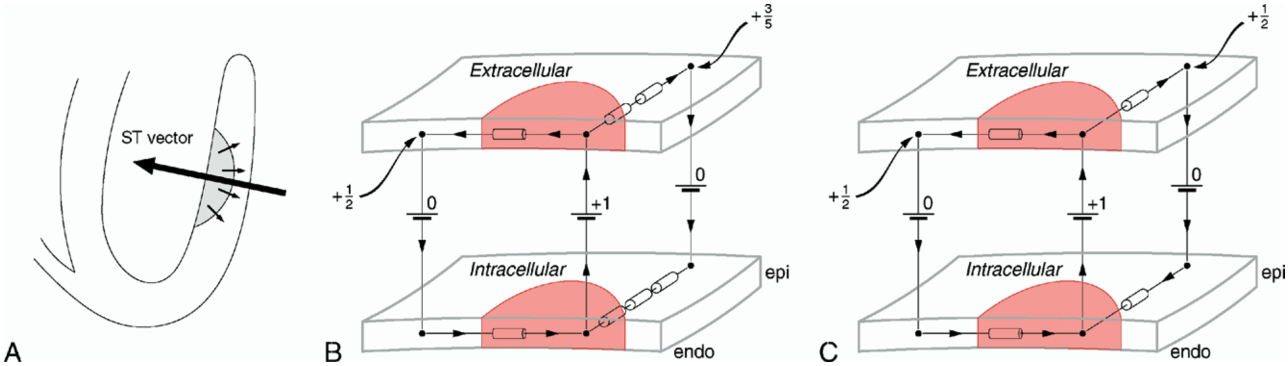

Figure 6 **A:** Classical explanation of ST depression in leads overlying a subendocardial ischemic zone. This description presumes isotropic tissue or at least a much reduced R_i. Thus, it presumes a large degree of tissue remodeling. **B:** Simple model to explain epicardial ST elevation in partial-thickness ischemia (see text for an explanation). **C:** A similar model showing that, in the absence of intracavitary blood, no ST deviation results in a fully isotropic heart.

Figure 6**B** explains ST elevation in epicardial leads overlying a subendocardial ischemia. For convenience, it will be described in terms of resistances rather than conductivities. The figure shows a transmural section of the ventricle. This section is shown twice: once for the intracellular and once for the extracellular domain. The shaded area indicates an ischemic zone. Its exact shape and size are unimportant in this treatment. Electric current is confined to a system of wires and resistors. All resistors have the same value; higher directional resistances are depicted with two or three resistors. The repartition of the resistors represent the fact that $R_i > R_e$. The cellular membrane is represented by potential sources, which have zero potential in the healthy tissue and unit potential in the ischemic area. The potential difference between the two areas then causes an extracellular current to flow from the ischemic to the healthy myocardium, returning through the intracellular domain. The current that passes through the epicardium encounters two resistors in the extracellular and three in the intracellular domain. Therefore, the potential at the epicardium is 3/5.

The current through the healthy endocardium encounters the same resistance in the intracellular as in the extracellular domain; hence the potential is 1/2 in the healthy endocardium. The extracellular potential is thus larger on the epicardium than on the healthy endocardium, which indicates an epicardial ST elevation. Figure 6**C** shows a similar model of isotropic tissue. In this case, no potential difference between the epicardial and lateral borders of the ischemia results. These predictions agree with the results of our more realistic model when the intracavitary blood is ignored (Figure 2). Both models predict ST depression when $R_i < R_e$. In a model where $R_i = R_e = 1$, epicardial ST depression occurs only due to the intracavitary blood.

Ischemia and remodeling

Myocardial ischemia often occurs with preexisting tissue remodeling, especially when it is chronic or recurrent. An important aspect of remodeling is the redistribution of gap junctions.[22] Gap junctions provide an electrically conducting pathway between cardiac myocytes. They are preferentially located in the intercalated disks (IDs). Gap junctions are formed by large proteins known as connexins. In human ventricular myocardium, connexin 43 (Cx43) is the most important of these.[37] Ischemia reduces the expression of phosphorylated Cx43[38,39] and gap-junctional area.[19] Reperfusion causes a return of phosphorylated Cx43, which is then more equally distributed along the membrane.[21,23] It is not known if the reappearing connexins are part of functional gap junctions. Both the disappearance of Cx43 from the ID and the formation of lateral gap junctions would contribute to reduced R_i. According to our results, this would favor ST depression (Figure 2). The conductivity of gap junctions is also modulated by pH and intracellular $[Ca^{2+}]$.[21,40] These factors too may be modified in ischemic myocardium, but they would only affect ST deviation if they change longitudinal and transverse conductivity differently (Figure 3). Reduction and lateralization of gap junctions have also been related to heart failure[24,41] and more specifically to hypertrophy.[19,20,22] Uzzaman et al[22] observed a 31% decrease in gap junction area in hypertrophic rat myocardium, with a reduction of anisotropy in propagation velocity. Cooklin et al[20] provided direct proof of reduced longitudinal conductivity.

ST deviation in experimental ischemia

Experimental studies of subendocardial ischemia demonstrated both ST elevation and ST depression on epicardium overlying a subendocardial ischemia. Guyton et al[13] found progressive epicardial ST depression during partial occlusion of the left circumflex artery (LCX) in dogs. Similarly, Hellerstein and Katz reported ST depression in epicardial leads overlying a zone of endocardial injury.[11] During occlusion of either the LCX or the left anterior descending artery (LAD), Li et al[14] found a zone of epicardial ST depression centered not on the ischemic area, but on its lateral border. Kilpatrick et al[15] showed that this negative zone is not displaced during a transition from subendocardial to transmural ischemia.

Results of this study

We found that ST depression on epicardium overlying a subendocardial ischemia can occur due to (1) reduced R_i, (2) increased R_e, and (3) a very large and thin ischemic zone. In other circumstances it leads to ST elevation on the overlying epicardium.[14–16,42] The finding that under some circumstances an ST depression is obtained in overlying leads may help to explain the results of early experimental studies, which found ST depression on the epicardium overlying a subendocardial ischemic or injured region.[11,13] A nontransmural ischemic zone large enough to provoke ST depression on the epicardium overlying its center has never been demonstrated in animal models. However, it may relate to the clinical presentation of circumferential subendocardial ischemia, which is characterized by ST depression in overlying precordial leads.[5,6]

The anisotropy in propagation velocity in cardiac tissue is promoted by both intracellular and extracellular anisotropic conductivity. In contrast, ST depression is favored by a decrease in R_i and by an increase in R_e. Thus, both factors may contribute to ST depression while cancelling their contributions to anisotropic propagation. Therefore, measurement of propagation velocity alone does not suffice to study the conductivity changes in ischemic or hypertrophic myocardium.

Comparison with other simulation studies

Several investigators have simulated ischemia, both with isotropic and anisotropic models.[14,16,17,43–46] Johnston et al[45] have explicitly pointed out the importance of anisotropy in mathematical models of ischemia. MacLachlan et al[17] have shown differences in transmural ST deviation patterns between isotropic and anisotropic myocardium for a heart embedded in a human torso. Early theoretical work using, by necessity, an isotropic myocardium, predicted ST elevation in transmural ischemia and ST depression in subendocardial ischemia.[47] Li et al[14] used an isotropic myocardium, but mimicked the effect of anisotropy by regional variation of the injury current. This study, as well as all later work using a more realistic anisotropic myocardium, predicted ST elevation even in subendocardial ischemia.[16] Depression was found over the lateral borders of the partial-thickness ischemia, the same location as in full-thickness ischemia.

Apart from the tissue conductivity values, the intracavitary blood influences ST deviation[48] (Figure 2). Johnston et al[45] predicted ST depression in a model study with a simplified anatomy using anisotropy ratios very close to ours, which may be due to the infinite blood mass used in their study. Recently, Hopenfeld et al[48] have shown ST depression overlying a subendocardial ischemia with 10% transmural extent. We have extended this finding for 30%–40% transmural extent and have shown that for larger diameters ST depression can be obtained with a larger transmural extent (Figure 5). In addition, we have shown how size and extent interact with R_i (Figure 5).

We have used a realistic profile of resting V_m based on assumptions on the extrusion and diffusion of K^+.[28] Regardless of the validity of these assumptions, the resulting profiles of $[K^+]_o$ and V_m resemble measured profiles[28,49] better than those used in earlier studies.[14,16,17,45]

Limitations

We have shown that all four bidomain conductivities play a role in determining ST deviation. Unfortunately, these values are not accurately known.[36] Measuring anisotropic bidomain conductivity is technically challenging and has only been done in papillary muscles.[50–52] Conductivity changes in ischemia have been measured, but anisotropy was not reported.[53] For a complete understanding of ST deviation, better estimates of these values are sorely needed.[15]

It is tempting to extrapolate our results to the ECG. This would allow comparison with many clinical and experimental studies. However, the relation between heart and surface potentials is complex. An anisotropic model of the heart coupled to an inhomogeneous torso model is required to predict ST deviation in the ECG.

Conclusion

In healthy myocardium, both transmural and compact subendocardial ischemic zones lead to epicardial ST elevation. Ischemia is likely to occur in tissue that is subject to a remodeling of anisotropic conductivity. We have shown that a reduction of R_i, an increase in R_e, or a sufficiently large and thin ischemic zone can explain ST depression in epicardial leads. These findings may help to explain the equivocal results that have been obtained in experimental endocardial ischemia or injury and to better understand the cause and nature of ST segment changes in clinical settings.

Acknowledgments

Several colleagues made important contributions to this paper through their comments and discussions. We would like to thank especially Dr. M. de Chantal, Dr. P. Savard, and Dr. R. Nadeau for reviewing our manuscript.

References

1. Antman EM, Braunwald E. ST-elevation myocardial infarction: pathology, pathophysiology, and clinical features. In: Zipes DP, Libby P, Bonow RO, Braunwald E, eds., Heart Disease, 7th ed. Elsevier Saunders, Philadelphia, PA, 2005:chapter 46.
2. Savonitto S, Ardissino D, Granger CB, Morando G, Prando MD, Mafrici A, Cavallini C, Melandri G, Thompson TD, Vahanian A, Ohman EM, Califf RM, Van de Werf F, Topol EJ. Prognostic value of the admission electrocardiogram in acute coronary syndromes. JAMA 1999;281:707–713.
3. Nyman I, Areskog M, Areskog NH, Swahn E, Wallentin L, the RISC Study Group. Very early risk stratification by electrocardiogram at rest in men with suspected unstable coronary heart disease. J Intern Med 1993;234:293–301.
4. Nasmith JB, Pharand C, Dubé B, Matteau S, LeBlanc AR, Nadeau R. Localization of maximal ST segment displacement in various ischemic settings by orthogonal ECG: implications for lead selection and the mechanism of ST shift. Can J Cardiol 2001;17:57–62.
5. Nikus KC, Eskola MJ, Niemelä KO, Sclarovsky S. How to use ECG for decision support in the catheterization laboratory; cases with ST-segment depression acute coronary syndrome. J Electrocardiol 2004;37:247–255.
6. Cook RW, Edwards JE, Pruitt RD. Electrocardiographic changes in acute subendocardial infarction. I. large subendocardial and large nontransmural infarcts. Circulation 1958;18:603–612.
7. Cannon CP, Braunwald E. Unstable angina and non-ST elevation myocardial infarction. In: Zipes DP, Libby P, Bonow RO, Braunwald E, eds., Heart Disease, 7th ed. Elsevier Saunders, Philadelphia, PA, 2005:chapter 49.

8. Mirvis DM, Ramanathan KB, Wilson JL. Regional blood flow correlates of ST segment depression in tachycardia-induced myocardial ischemia. Circulation 1986;73:365–373.
9. Vincent GM, Abildskov JA, Burgess MJ. Mechanisms of ischemic ST-segment displacement: evaluation by direct current recordings. Circulation 1977;56:559–566.
10. Katcher AH, Peirce G, Sayen JJ. Effects of experimental regional ischemia and levarterenol on the RS-T segment and baseline of ventricular surface electrocardiograms obtained by direct-coupled amplification. Circ Res 1960;8:29–43.
11. Hellerstein HK, Katz LN. The electrical effects of injury at various myocardial locations. Am Heart J 1948;36:184–220.
12. Kléber AG, Janse MJ, van Capelle FJL, Durrer D. Mechanism and time course of S-T and T-Q segment changes during acute regional myocardial ischemia in the pig heart determined by extracellular and intracellular recordings. Circ Res 1978;42:603–613.
13. Guyton RA, McClenathan JH, Newman GE, Michaelis LL. Significance of subendocardial S-T segment elevation caused by coronary stenosis in the dog. Epicardial S-T segment depression, local ischemia and subsequent necrosis. Am J Cardiol 1977;40:373–380.
14. Li D, Li CY, Yong AC, Kilpatrick D. Source of electrocardiographic ST changes in subendocardial ischemia. Circ Res 1998;82:957–970.
15. Kilpatrick D, Johnston PR, Li DS. Mechanisms of ST change in partial thickness ischemia. J Electrocardiol 2003;36(Suppl):7–12.
16. Hopenfeld B, Stinstra JG, MacLeod RS. Mechanism for ST depression associated with contiguous subendocardial ischemia. J Cardiovasc Electrophysiol 2004;15:1200–1206.
17. MacLachlan MC, Sundnes J, Lines GT. Simulation of ST segment changes during subendocardial ischemia using a realistic 3-D cardiac geometry. IEEE Trans Biomed Eng 2005;52:799–807.
18. Kléber AG, Riegger CB, Janse MJ. Electrical uncoupling and increase of extracellular resistance after induction of ischemia in isolated, arterially perfused rabbit papillary muscle. Circ Res 1987;61:271–279.
19. Peters NS, Green CR, Poole-Wilson PA, Severs NJ. Reduced content of connexin43 gap junctions in ventricular myocardium from hypertrophied and ischemic human hearts. Circulation 1993;88:864–875.
20. Cooklin M, Wallis WRJ, Sheridan DJ, Fry CH. Changes in cell-to-cell electrical coupling associated with left ventricular hypertrophy. Circ Res 1997;80:765–771.
21. Jongsma HJ, Wilders R. Gap junctions in cardiovascular disease. Circ Res 2000;86:1193–1197.
22. Uzzaman M, Honjo H, Takagishi Y, Emdad L, Magee AI, Severs NJ, Kodama I. Remodeling of gap junctional coupling in hypertrophied right ventricles of rats with monocrotaline-induced pulmonary hypertension. Circ Res 2000;86:871–878.
23. Daleau P, Boudriau S, Michaud M, Jolicoeur C, Kingma JG. Preconditioning in the absence or presence of sustained ischemia modulates myocardial Cx43 protein levels and gap junction distribution. Can J Physiol Pharmacol 2001;79:371–378.
24. Poelzing S, Rosenbaum DS. Altered connexin43 expression produces arrhythmia substrate in heart failure. Am J Physiol Heart Circ Physiol 2004;287:H1762–H1770.
25. Potse M, Dubé B, Richer J, Vinet A, Gulrajani RM. A comparison of monodomain and bidomain reaction-diffusion models for action potential propagation in the human heart. IEEE Trans Biomed Eng 2006;53:2425–2435.
26. Miller WT III, Geselowitz DB. Simulation studies of the electrocardiogram. I. The normal heart. Circ Res 1978;43:301–315.
27. Henriquez CS. Simulating the electrical behavior of cardiac tissue using the bidomain model. CRC Crit Rev Biomed Eng 1993;21:1–77.
28. Coronel R, Fiolet JWT, Wilms-Schopman FJG, Schaapherder AFM, Johnson TA, Gettes LS, Janse MJ. Distribution of extracellular potassium and its relation to electrophysiologic changes during acute myocardial ischemia in the isolated perfused porcine heart. Circulation 1988;77:1125–1138.
29. Rodríguez B, Ferrero JM Jr, Trénor B. Mechanistic investigation of extracellular K+ accumulation during acute myocardial ischemia: a simulation study. Am J Physiol Heart Circ Physiol 2002;283:H490–H500.
30. Janse MJ, Cinca J, Moréna H, Fiolet JWT, Kléber AG, de Vries GP, Becker AE, Durrer D. The "border zone" in myocardial ischemia: an electrophysiological, metabolic, and histochemical correlation in the pig heart. Circ Res 1979;44:576–588.
31. Yellon DM, Hearse DJ, Crome R, Grannell J, Wyse RKH. Characterization of the lateral interface between normal and ischemic tissue in the canine heart during evolving myocardial infarction. Am J Cardiol 1981;47:1233–1239.
32. Kléber AG, Fleischhauer J, Cascio WE. Ischemia-induced propagation failure in the heart. In: Zipes DP, Jalife J, eds., Cardiac electrophysiology: from cell to bedside, 2d ed. Saunders, Philadelphia, PA, 1995:chapter 19.
33. Gulrajani RM. Bioelectricity and Biomagnetism. Wiley, New York, 1998.
34. ten Tusscher KHWJ, Noble D, Noble PJ, Panfilov AV. A model for human ventricular tissue. Am J Physiol Heart Circ Physiol 2004;286:H1573–H1589.
35. Neu JC, Krassowska W. Homogenization of syncytial tissues. Crit Rev Biomed Eng 1993;21:137–199.
36. Roth BJ. Electrical conductivity values used with the bidomain model of cardiac tissue. IEEE Trans Biomed Eng 1997;44:326–328.
37. Thomas SA, Schuessler RB, Berul CI, Beardslee MA, Beyer EC, Mendelsohn ME, Saffitz JE. Disparate effects of deficient expression of connexin43 on atrial and ventricular conduction: evidence for chamber-specific molecular determinants of conduction. Circulation 1998;97:686–691.
38. Beardslee MA, Lerner DL, Tadros PN, Laing JG, Beyer EC, Yamada KA, Kléber AG, Schuessler RB, Saffitz JE. Dephosphorylation and intracellular redistribution of ventricular connexin43 during electrical uncoupling induced by ischemia. Circ Res 2000;87:656–662.
39. Ando M, Katare RG, Kakinuma Y, Zhang D, Yamasaki F, Muramoto K, Sato T. Efferent vagal nerve stimulation protects heart against ischemia-induced arrhythmias by preserving connexin43 protein. Circulation 2005;112:164–170.
40. van Veen TAB, van Rijen HVM, Jongsma HJ. Electrical conductance of mouse connexin45 gap junction channels is modulated by phosphorylation. Cardiovasc Res 2000;46:496–510.
41. de Groot JR, Coronel R. Acute ischemia-induced gap junctional uncoupling and arrhythmogenesis. Cardiovasc Res 2004;62:323–334.
42. Cinca J, Warren M, Carreño A, Tresànchez M, Armadans L, Gómez P, Soler-Soler J. Changes in myocardial electrical impedance induced by coronary artery occlusion in pigs with and without preconditioning; correlation with local ST-segment potential and ventricular arrhythmias. Circulation 1997;96:3079–3086.
43. Dubé B, Gulrajani RM, Lorange M, LeBlanc AR, Nasmith J, Nadeau RA. A computer heart model incorporating anisotropic propagation. IV. Simulation of regional myocardial ischemia. J Electrocardiol 1996;29:91–103.
44. Li D, Li CY, Yong AC, Johnston PR, Kilpatrick D. Epicardial ST depression in acute myocardial infarction. Circ Res 1999;85:959–964.
45. Johnston PR, Kilpatrick D, Li CY. The importance of anisotropy in modeling ST segment shift in subendocardial ischaemia. IEEE Trans Biomed Eng 2001;48:1366–1376.
46. Johnston PR. The effect of simplifying assumptions in the bidomain model of cardiac tissue: application to ST segment shifts during partial ischaemia. Math Biosci 2005;198:97–118.
47. Holland RP, Brooks H, Lidl B. Spatial and nonspatial influences on the TQ-ST segment deflection of ischemia. J Clin Invest 1977;60:197–214.
48. Hopenfeld B, Stinstra JG, MacLeod RS. The effect of conductivity on ST-segment epicardial potentials arising from subendocardial ischemia. Ann Biomed Eng 2005;33:751–763.
49. Coronel R, Wilms-Schopman FJG, Opthof T, van Capelle FJL, Janse MJ. Injury current and gradients of diastolic stimulation threshold, TQ potential, and extracellular potassium concentration during acute regional ischemia in the isolated perfused pig heart. Circ Res 1991;68:1241–1249.
50. Le Guyader P, Trelles F, Savard P. Extracellular measurement of anisotropic bidomain myocardial conductivities. I. Theoretical analysis. Ann Biomed Eng 2001;29:862–877.
51. Johnston BM, Johnston PR, Kilpatrick D. Analysis of electrode configurations for measuring cardiac tissue conductivities and fibre rotation. Ann Biomed Eng 2006;34:986–996.
52. Pollard AE, Barr RC. Cardiac microimpedance measurement in two-dimensional models using multisite interstitial stimulation. Am J Physiol Heart Circ Physiol 2006;290:H1976–1987.
53. Salazar Y, Bragos R, Casas O, Cinca J, Rosell J. Transmural versus nontransmural *in situ* electrical impedance spectrum for healthy, ischemic, and healed myocardium. IEEE Trans Biomed Eng 2004;51:1421–1427.
54. Rush S, Abildskov JA, McFee R. Resistivity of body tissues at low frequencies. Circ Res 1963;12:40–50.